

FULLY TRANSPARENT METAMATERIAL AMC BACKED CPW FED MONOPOLE ANTENNA FOR IOT APPLICATIONS

Cong Danh Bui^{1,2}, Arpan Desai^{1,2}, Thi Thanh Kieu Nguyen³,
Truong Khang Nguyen^{1,2,*}

¹*Division of Computational Physics, Institute for Computational Science,
Ton Duc Thang University, District 7, Ho Chi Minh City 70000, Viet Nam*

²*Faculty of Electrical and Electronics Engineering, Ton Duc Thang University, District 7,
Ho Chi Minh City 70000, Viet Nam*

³*Department of Electronics, Binh Thuan Province Vocational College, Binh Thuan Province,
Phan Thiet City 77000, Viet Nam*

*Emails: nguyentruongkhang@tdtu.edu.vn

Received: 25 January 2021; Accepted for publication: 9 September 2021

Abstract. In this paper, a fully transparent antenna comprising of an Artificial Magnetic Conductor (AMC) backed Co-planar Waveguide (CPW) fed dual-ring monopole is presented. The monopole antenna and AMC structure achieve transparency due to the use of AgHT-8 conductive oxide and Plexiglas substrate. Measured antenna performance shows an impedance bandwidth of 5.3 – 6 GHz (12.4 %) in the U-NII-1 to U-NII-4 frequency band with a peak gain of 5.7 dBi which is approximately an increase of 4.5 % and 3.9 dBi, respectively, as compared to the stand-alone antenna. The simulation and the measurement results agree well with each other which proves the validity of the proposed design. To the best of our knowledge, the proposed antenna is the first fully transparent antenna design combining a transparent radiator and a transparent AMC structure.

Keywords: Transparent antenna, monopole, AgHT, AMC, Plexiglas.

Classification numbers: 2.1.2, 4.1.1

1. INTRODUCTION

Monopole antenna is one of the most widely used antenna types in modern technology as it is simple, low cost, and suitable for multiple commercial applications [1, 2]. Despite having a compact size and low - profile, the planar monopole antenna suffers from low radiation efficiency because the main electric component has its radiation canceled by staying on the same plane as the ground plane [3]. Metamaterials are an interesting research topic because antenna performance (e.g. bandwidth, gain, size) can be improved with appropriate implementation [4 - 6]. AMC, a type of metamaterial, is a well-known technique to improve gain performance by placing on the backside of the antenna. The AMC structure consists of multiple unit cells that are duplicated along with its fixed periodicity and have its operating bandwidth defined where the reflection phase of the unit cell model is ranged from 90° to -90° [7]. It makes the antenna design

more complex as the topology of the unit cell, which is the core of the AMC structure, strongly depends on its shape and size but the improvement in bandwidth and gain compared to the stand-alone antenna is also adequate. There are many published works regarding AMC-backed antenna design. In [8], a bowtie antenna that was backed by 9×6 unit cells of the circular patch was proposed. The antenna has a relatively small size of $75 \times 110 \text{ mm}^2$ over the bandwidth from 1.64 - 1.94 GHz (16.7 %). The main disadvantage of the design was the low gain (6.5 dBi) as compared to the gain reported in [9] (10.1 dBi), where Pooja Prakash *et al.* introduced a ring slot AMC unit cell in a 4×4 AMC array to improve gain for a rectangular monopole antenna. Though the antenna in [9] exhibited a wider bandwidth of 4.25 - 6.9 GHz (47.53 %), its overall dimension in terms of wavelength was larger than that of the antenna proposed in [8].

Recent advances in technology have greatly reduced the size of IoT devices. The main disadvantage of using an AMC structure at the back of the antenna results in the consumption of useful board space due to the distance between the antenna and the AMC structure. If the antenna is made transparent, it can be installed anywhere within the device without occupying the functional space of other electronic components. Transparent antennas can be installed anywhere in the room, most ideally on transparent surfaces such as windows, glasses, overhead lights, etc. There are 2 main ways to achieve a transparent antenna, that is using metal mesh or transparent material. In the metal mesh approach, transparency is achieved through gaps in the copper mesh [10, 11]. Although the antenna performance is good, the transparency is much lower than when using transparent material. Transparent materials such as Plexiglas substrates or AgHT conductive sheets with greater than 75 % transparency are widely used for transparent antennas despite their low conductivity. This problem leads to low efficiency and gain, which can be overcome by using the AMC structure. However, to our knowledge, even though there is a transparent monopole antenna by using metal mesh [12] or optically transparent material [13], the use of AMC structure for this type of antenna is still limited.

Furthermore, the extreme rise in data ingestion requires Wi-Fi to operate at high speeds, driven by new applications, devices, and use cases. The Unlicensed International Infrastructure (U-NII) radio band, which is a part of IEEE 802.11a, offers a new spectrum. This spectrum especially operates over 4 bands: from U-NII-1 to U-NII-4 which ranges from 5.15 GHz to 5.925 GHz [14], making it suitable for many indoor and outdoor uses as well as Dedicated Short Range Communication applications [15].

Therefore, this paper proposes a transparent dual ring monopole antenna with AMC support, operating in the spectrum range from U-NII-1 to U-NII-4 (5.15 - 5.925 GHz). The AMC unit cell design and its effect on antenna bandwidth and gain are discussed in Section II. Section III shows the simulation and measurement results of the proposed design using CST software. Finally, conclusions on the antenna is given in Section IV.

2. ANTENNA GEOMETRY AND PARAMETRIC STUDY

The dual ring CPW based transparent antenna geometry is illustrated in Fig. 1 (a,b) [16]. The antenna structure achieves transparency by using conductive oxide AgHT-8 and Plexiglas where AgHT-8 has a thickness and plate impedance of 0.177 mm and $8\Omega/\text{sq}$, respectively.

The designed transparent antenna is interfaced with an AMC structure that has 4×4 -unit cells and is held below the antenna at an optimized distance (d) as shown in Fig. 1 (c, d). The artificial magnetic conductor (AMC) consists of three layers including the top layer of a 4×4 -unit cell array formed using AgHT-8, a middle layer made up of Plexiglas substrate, and a

bottom layer as the ground plane with a total thickness of $T = 1.83$ mm. The optimized antenna dimensions of the dual ring antenna are shown in Table 1.

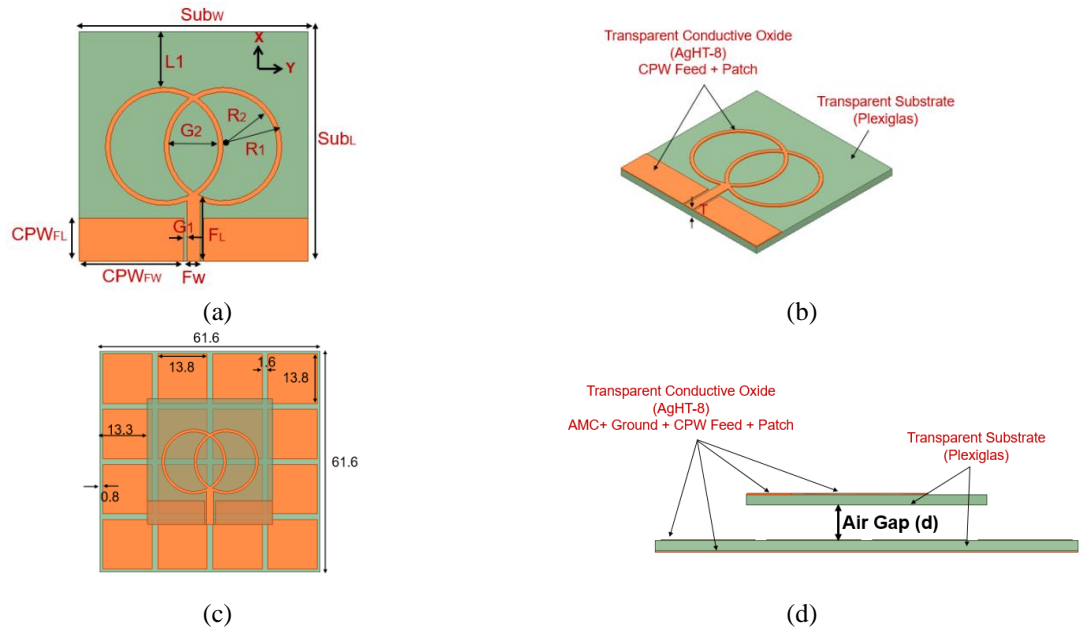


Figure 1. Antenna geometry: (a) top view of the radiator without AMC (b) Perspective view without AMC (c) top view of the radiator with AMC (d) Side view with AMC (Dimensions are in mm).

Table 1. Dimensions of Transparent Antenna.

Antenna Parameters	Dimensions (in mm)	Antenna Parameters	Dimensions (in mm)
$SubW = SubL$	35	$L1$	8.5
CPW_{FL}	6.5	$G1$	0.5
CPW_{FW}	16	$G2$	7.6
F_w	2	$R1$	9
F_L	9.208	$R2$	8.3
d	5	T	1.83

Figure 2 (a) depicts the internal radius variation of the hollow circular ring. As the radius decreases the frequency band shifts towards the lower side and the reflection coefficient decreases, while the opposite happens as the radius increases. For best results, the size of the radius ($R2$) was chosen to be 8.3 mm.

The variation of the gap between the CPW feed and the microstrip line ($G1$) affects the impedance bandwidth of the antenna. As the gap decreases, the impedance bandwidth increases as can be seen in Fig. 2 (b). The optimum gap between the CPW feed and the microstrip line is carefully chosen to be 0.5 mm for more precise fabrication.

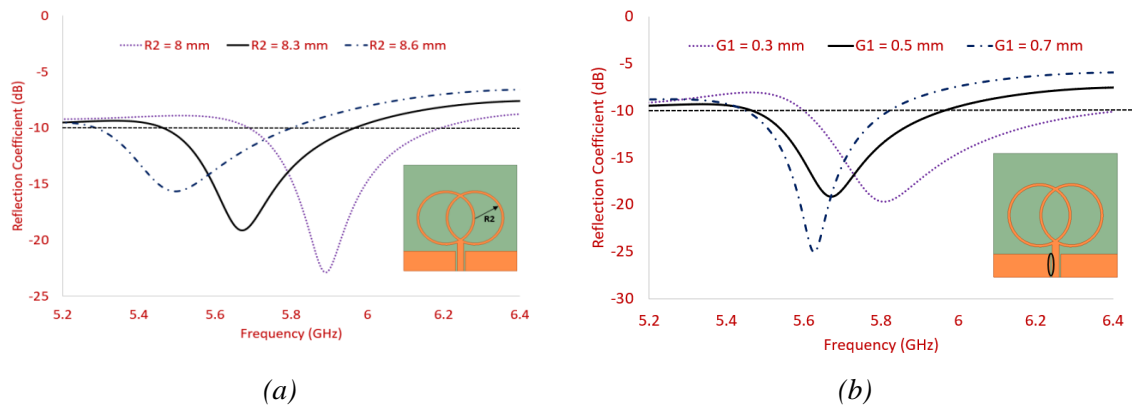


Figure 2. Parametric Variation of a hollow circular ring (a) Inner radius (R2) (b) gap between CPW feed and microstrip line (G1).

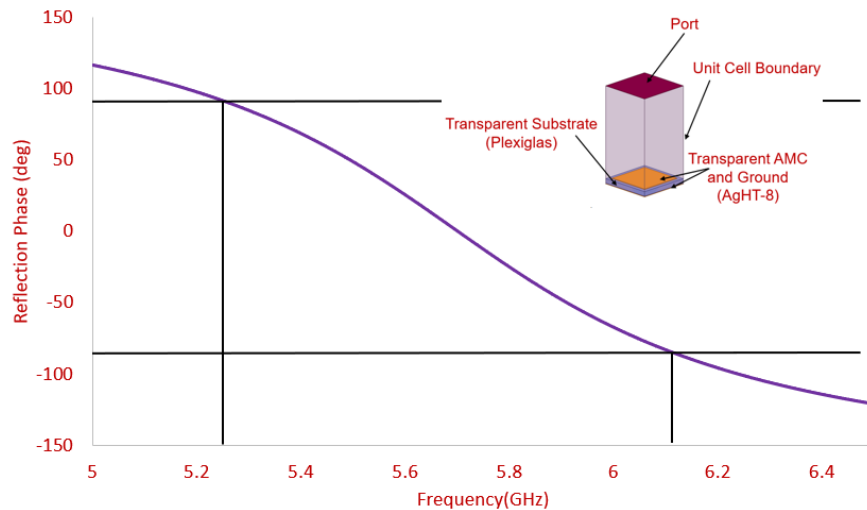


Figure 3. Reflection Phase of Single AMC Structure.

The AMC simulation model consists of an AMC unit cell enclosed inside a unit cell boundary and provided the feed from the top side. The reflection phase illustrates that the in-phase region of the frequency range 5.3 - 6.2 GHz is spanned between $\pm 90^\circ$ as shown in Fig. 3.

The effect on $|S_{11}|$ and gain is analyzed by varying the AMC distance from the transparent radiator as shown in Fig. 4 (a, b). As the air gap between the antenna and the AMC structure increases, the impedance bandwidth decreases while the reflection coefficient improves greatly. A value of air gap distance (d) of 5 mm shows the maximum impedance bandwidth as compared to the radiator with AMC distance of 0 mm and 10 mm, respectively. The gain plot as shown in Fig. 4(b) depicts that the AMC at a distance of 5 mm from the transparent radiator shows an average gain of more than 5 dBi for the proposed bands. The value of gain is negative for frequencies lower than 5.56 GHz when the distance (d) is 0 mm and positive gain is obtained when the value of d is 10 mm. However, the gain value is still smaller than that achieved for d = 5 mm.

The mean E-field distribution at 5.67 GHz is plotted as shown in Fig. 5 by varying the distance between the AMC and the transparent radiator. It can be seen that when d = 5 mm (Fig.

5b), the E-field distribution on the AMC is not only spread out evenly on all sides but also concentrated on the dual ring, which is the main radiating element. When $d = 0$ mm, the electric field magnitude on the lower side of the AMC is very weak, opposite to the case of $d = 10$ mm.

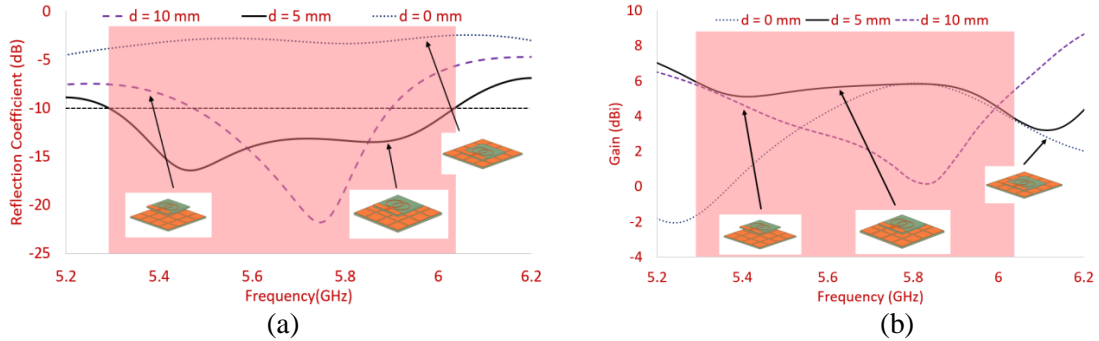


Figure 4. Performance of the proposed antenna due to AMC distance from single antenna (a) $|S_{11}|$ (b) Gain.

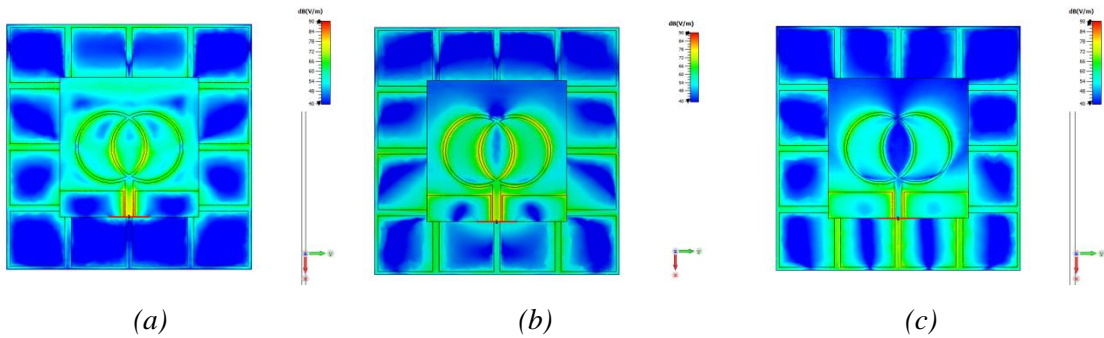


Figure 5. Average E-field distribution at 5.67 GHz with respect to difference antenna-AMC distances (a) $d = 0$ mm (b) $d = 5$ mm (c) $d = 10$ mm.

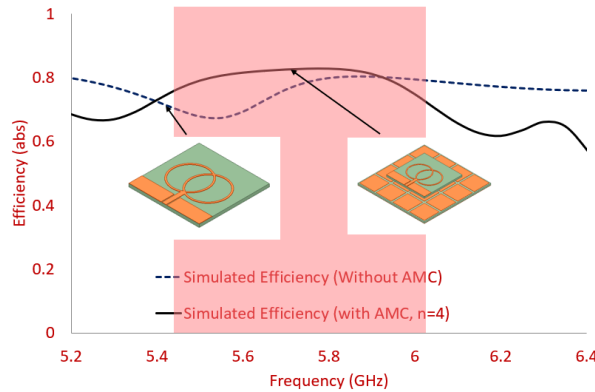


Figure 6. Performance of Transparent antenna in terms of Efficiency.

Furthermore, regarding the magnitude of the electric field, the distribution on the dual ring is not high in the case of $d = 0$ mm and relatively low, especially in the central area, in the case of $d = 10$ mm when compared with the case of $d = 5$ mm. The air gap distance $d = 5$ mm shows not only the strong distribution on both the dual ring monopole and the AMC structure, but also the uniformity on the surface of the AMC structure. Therefore, the value of the air gap distance is chosen to be 5 mm.

It is observed from Fig. 6 that a transparent antenna achieves higher efficiency in the operating bandwidth with AMC than an antenna without AMC.

3. RESULTS AND DISCUSSION

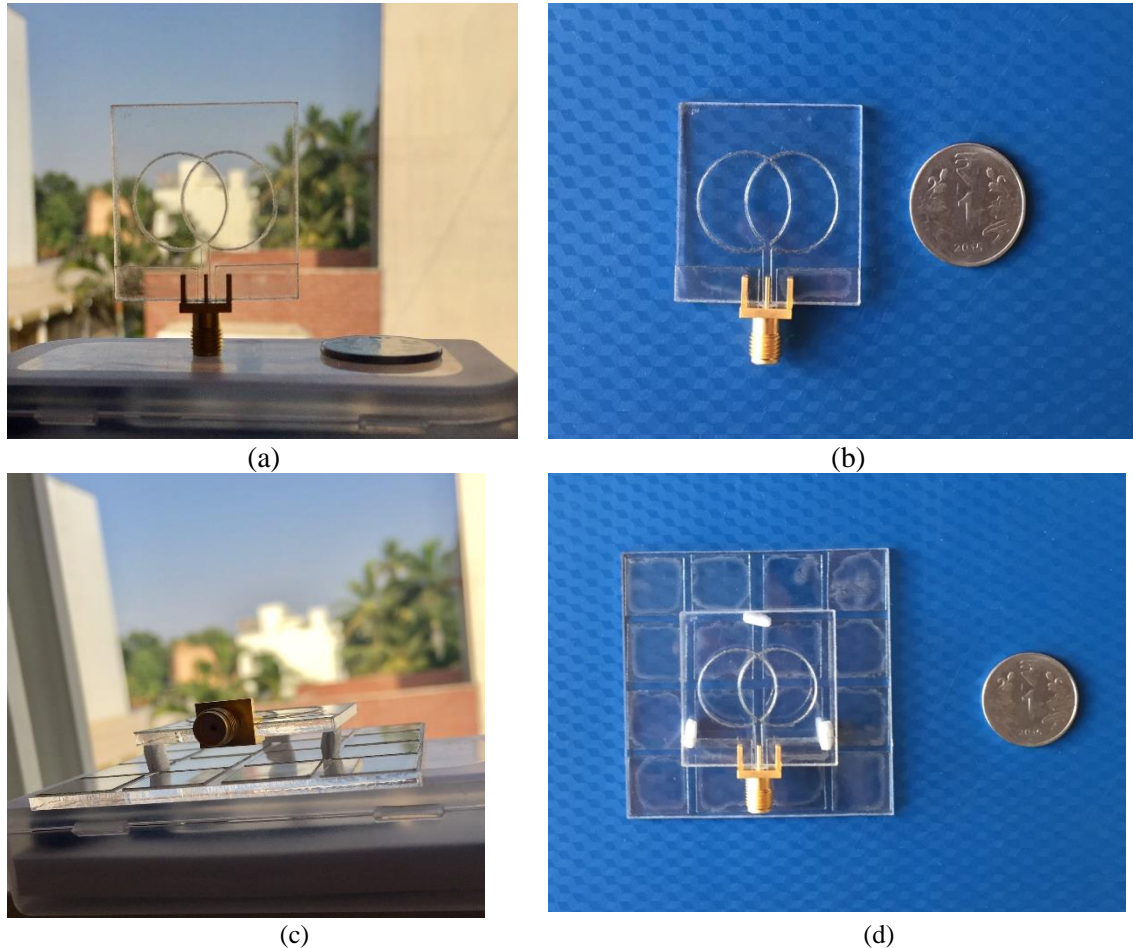


Figure 7. Fabricated Antenna: (a) front view of the radiator without AMC (b) top view without AMC (c) front view of the radiator with AMC (d) Side view with AMC.

The fabricated transparent radiator front and top views are depicted in Fig. 7 (a, b). A transparent antenna with AMC structure at a distance of 5 mm is fabricated by using Styrofoam columns ($\epsilon_r = 1$) in the middle to create the required air gap. The side and top views of the antenna with AMC are visible in Fig. 7 (c, d).

The fabricated antennas, both with and without AMC structure, have been tested for reflection coefficient. The measured frequency band of the single element fabricated antenna spans from (7.55 %) 5.48 to 5.91 GHz, which is in good correlation with the simulated value ranging from (8.8 %) 5.46 to 5.96 GHz as observed from Fig. 8 (a). The antenna with AMC resonates in the frequency range of (12.01 %) 5.32 - 6.0 GHz, close to the simulated value spanning from (13.06 %) 5.292 to 6.032 GHz as observed from Fig. 8 (b). The simulation results and the measured results are in good agreement with each other due to the precise fabrication

technique used to achieve the desired shape of the monopole which is performed using the simulation. The antenna geometry is patterned using a laser cutter to achieve the utmost precision. An extra thin double-sided adhesive sheet is used to stick the conductive sheet with the substrate. The main purpose of using this method is to avoid air gaps that can occur if conventional adhesives are used. The low-loss SMA connector is interfaced with the antenna using a conductive adhesive (Silver/Graphene paste) instead of hot solder. Finally, the VNA and the anechoic chamber used for measurement are calibrated and used under conditions of very low noise levels at IF (intermediate frequency) bandwidth.

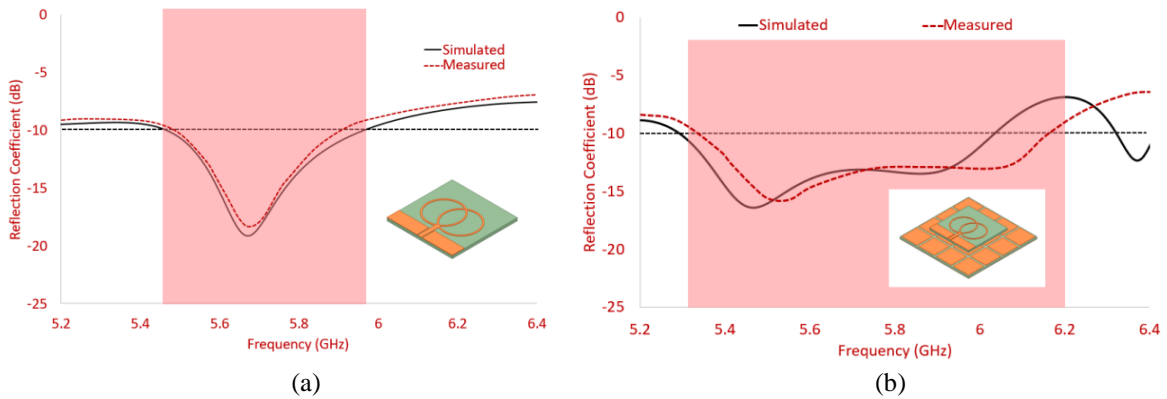


Figure 8. Performance of Transparent antenna in terms of $|S_{11}|$ (a) without AMC (b) with AMC.

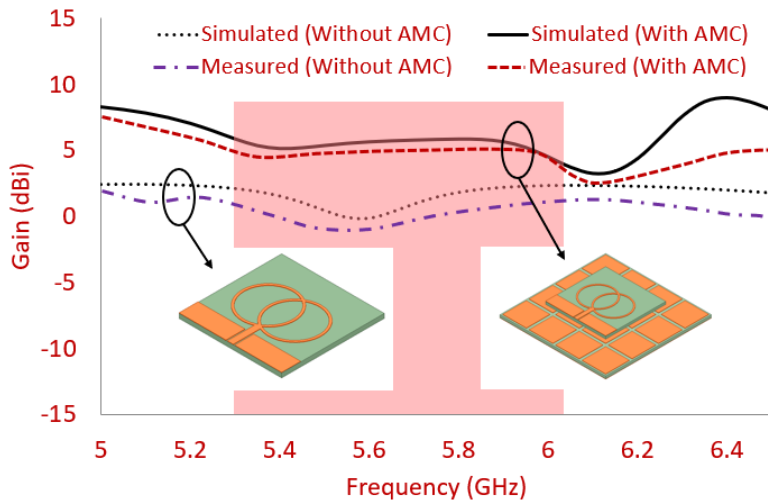


Figure 9. Performance of Transparent antenna in terms of Gain.

The performance of the antenna with AMC in terms of gain is depicted in Fig. 9, where it can be observed that a stand-alone transparent antenna shows a lower value of gain as compared to the antenna with a 4×4 AMC array at the back. This is significant since the AMC structure makes the radiation pattern more directive, thus helping to achieve more gain. The antenna shows an average gain in the range of 5.47 dBi for the proposed band.

The radiation patterns for the E and H planes depicted in Fig. 10 (a, b) at 5.5 GHz and 5.85 GHz, respectively, were measured in an anechoic chamber. The back lobes are greatly reduced in the antenna with the AMC structure, which helps to make the radiation patterns more

directional. Therefore, it enhances the gain of the antenna. The setup for measuring the radiation pattern and gain in anechoic chamber is shown in Fig. 11.

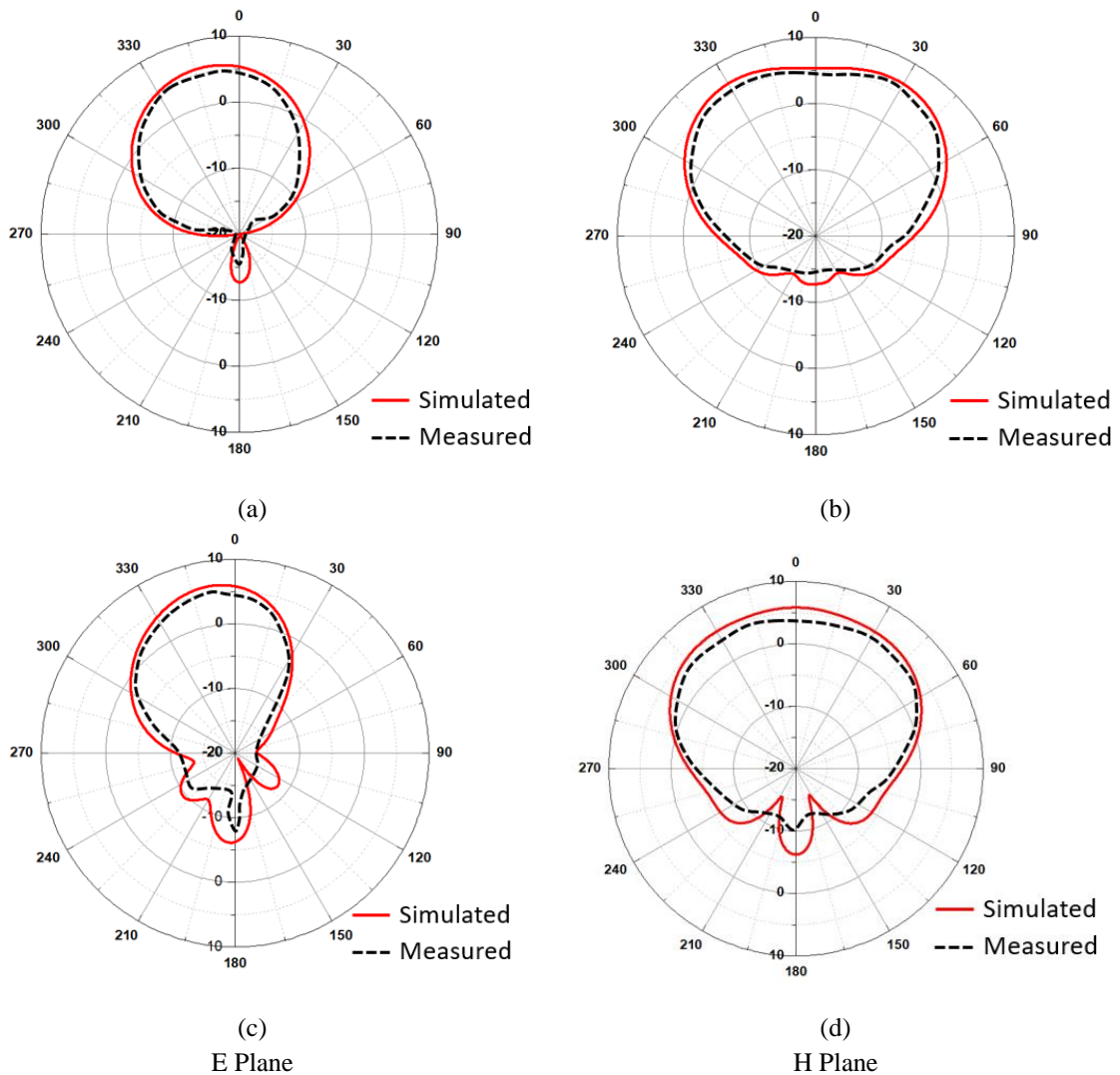


Figure 10. 2D radiation pattern (Simulated and Measured) of the proposed antenna at (a) 5.5 GHz (b) 5.85 GHz.

Table 2 shows a comparison of the proposed design with the previously published monopole antenna designs. In general, published designs are divided into antennas having either transparency [13, 19 - 20], or AMC structure [9, 17 - 18]. AMC-backed monopole antenna has the advantage of high gain despite its much larger average size than transparent antennas. On the other hand, transparent antennas have a wider fractional impedance bandwidth by using a radiator structure, but low gain performance is inevitable due to the inherently low conductivity of the material. To the best of our knowledge, the proposed antenna is the first to combine a transparent material with an AMC structure. The design has high gain and comparable size and fractional bandwidth making it suitable for many IoT applications.

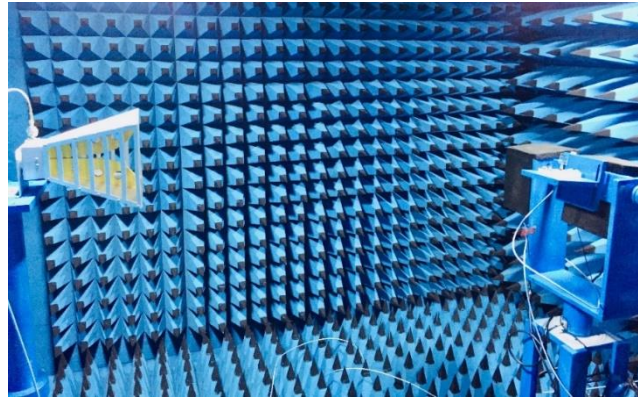


Figure 11. Antenna Setup in Anechoic Chamber.

Table 2. Comparison of AMC based transparent antenna with other AMC based antennas from literature.

References	Size (λ_0^3)	Bandwidth	Gain (dBi)	Transparency	AMC
[9]	$1.27 \times 1.27 \times 0.4$	4.25 - 6.9 GHz (47.53 %)	10.1	No	Yes
[13]	$0.17 \times 0.17 \times 0.004$	1 - 7 GHz (150 %)	-4	Yes	No
[17]	$0.55 \times 0.55 \times 0.03$	1.83 - 1.97 GHz (7.03 %)	4.3	No	Yes
[18]	$0.63 \times 0.81 \times 0.08$	4.67 - 6.41 GHz (31.4 %)	5.61	No	Yes
[19]	$0.31 \times 0.46 \times 0.002$	3.15 - 32 GHz (164 %)	-3.2	Yes	No
[20]	$0.45 \times 0.3 \times 0.01$	1.5 - 4.0 GHz (90.91 %)	3.16	Yes	No
Proposed	$1.1 \times 1.1 \times 0.14$	5.3 - 6 GHz (12.4 %)	5.7	Yes	Yes

Note: λ_0 is the wavelength at the lowest frequency

4. CONCLUSIONS

A 4×4 metamaterial array-backed transparent antenna with a dual-ring structure is proposed. Complete transparency is achieved by the use of AgHT-8 and Plexiglas as transparent conductive oxides and substrate, and AMC, respectively. Analysis of distance between AMC cell arrays and the transparent radiator is carried out to improve the impedance bandwidth and gain of the antenna. The AMC structure with a 4×4 array size at a distance of 5 mm from the main radiator shows the maximum value of gain and bandwidth, causing an increase of 3.9 dBi and 4.5 %, respectively as compared to the stand-alone antenna. The transparency coupled with the enhanced performance in gain, bandwidth and directional radiation pattern make the proposed AMC-backed antenna suitable for use in the spectral range from U-NII-1 to U-NII-4.

Acknowledgements. This research is funded by Vietnam National Foundation for Science and Technology Development (NAFOSTED) under grant number 102.04-2019.04.

Credit authorship contribution statement. C. D. Bui, A. Desai: Methodology, Investigation, Formal analysis, Writing. T. T. K. Nguyen: Editing, Formal analysis. T. K. Nguyen: Writing, Editing, Supervision.

Declaration of competing interest. The authors declare that they have no known competing financial interests or personal relationships that could have appeared to influence the work reported in this paper.

REFERENCES

1. Liang J., Chiau C., Chen X., and Parini C. - Printed circular disc monopole antenna for ultra-wideband applications, *Electronics Letters* **40** (20) (2004) 1246-1247. 10.1049/el:20045966.
2. Pan C. Y., Horng T. S., Chen. W. S., and Huang C. H. - Dual wideband printed monopole antenna for WLAN/WiMAX applications, *IEEE Antennas and Wireless Propagation Letters* **6** (2007) 149-151. 10.1109/LAWP.2007.891957.
3. Balanis C. A. - *Antenna Theory: Analysis and Design*, 4th ed. John Wiley & Sons, 2016, pp. 207-208.
4. Phan D. T., Phan H. L., Nguyen T. Q. H. - A miniaturization of microstrip antenna using negative permittivity metamaterial based on CSRR-loaded ground for WLAN applications, *Vietnam Journal of Science and Technology* **54** (6) (2016) 689-697. 0.15625/0866-708X/54/6/8375.
5. Ullah S., Phan H. L., Phan D. T., Tran S. T., Nguyen T. Q. H. - Design and analysis of compact metamaterial MIMO antenna for WLAN applications, *Vietnam Journal of Science and Technology* **57** (2) (2019) 223-232. <https://doi.org/10.15625/2525-2518/57/2/12992>.
6. Dang N. D., Dinh T. L., Huynh N. B., Hoang P. C., Dao N. C. - Novel compact dual-broadband planar metamaterial antenna, *Vietnam Journal of Science and Technology* **55** (3) (2017) 334-346. 10.15625/2525-2518/55/3/8569.
7. Dewan R., Rahim M. K., et al. - Artificial magnetic conductor for various antenna applications: An overview, *Int. J. RF Microw. Comput. Aided Eng.* **27** (6) (8/2017), Art. no. e21105. <https://doi.org/10.1002/mmce.21105>.
8. Zhong Y. W., Yang G. M., and Zhong L. R. - Gain enhancement of bowtie antenna using fractal wideband artificial magnetic conductor ground, *Electronics Letters* **51** (4) (2015) 315-317. <https://doi.org/10.1049/el.2014.4017>.
9. Prakash P., Abegaonkar M. P., Basu A., and Koul S. K. - Gain enhancement of a CPW-fed monopole antenna using polarization-insensitive AMC structure, *IEEE Antennas and Wireless Propagation Letters* **12** (2013) 1315-1318. 10.1109/LAWP.2013.2285121.
10. Kang S. H. and Jung C. W. - Transparent patch antenna using metal mesh, *IEEE Transactions on Antennas and Propagation* **66** (4) (2018) 2095-2100. 10.1109/TAP.2018.2804622.
11. Hong S., Kim Y., and Jung C. W. - Transparent microstrip patch antennas with multilayer and metal-mesh films, *IEEE Antennas and Wireless Propagation Letters* **16** (2016) 772-775. 10.1109/LAWP.2016.2602389.
12. Lee J. H., Lee S. H., Kim D., and Jung C. W. - Transparent dual-band monopole antenna using a μ -metal mesh on the rear glass of an automobile for frequency modulation/digital media broadcasting service receiving, *Microwave and Optical Technology Letters* **61** (2) (2019) 503-508. <https://doi.org/10.1002/mop.31567>.

13. Cai L. - An on-glass optically transparent monopole antenna with ultrawide band width for solar energy harvesting, *Electronics* **8** (9) (2019) 916.
<https://doi.org/10.3390/electronics8090916>.
14. Commission F. C., *et al.* - Unlicensed national information infrastructure (U-NII) devices in the 5 GHz band, et docket no. 13-49, FCC 16-68, FCC **81** (109) (6/2016) 36501-36506.
15. Kim. S and Kim. B. J. - Crash risk-based prioritization of basic safety message in DSRC, *IEEE Access* **8** (2020) 211961-211972. 10.1109/ACCESS.2020.3039516.
16. Bui C. D, Desai A., and Nguyen T. K. - A Design of ISM Band Transparent Metamaterials backed Dual Ring CPW Fed Antenna for IoT Applications, In 2020 IEEE Eighth International Conference on Communications and Electronics (ICCE), 2021, pp. 186-190. 10.1109/ICCE48956.2021.9352108.
17. Andriamiharivolamena T., Lemaître-Auger P., Tedjini S., and Tirard F. - Compact planar monopole antenna for wearable wireless applications, *Comptes Rendus Physique* **16** (9) (2015) 851-861. <https://doi.org/10.1016/j.crhy.2015.07.008>.
18. Dewan R., Rahim S. K. B. A., Ausordin S. F., and Purnamirza T. - The improvement of array antenna performance with the implementation of an artificial magnetic conductor (AMC) ground plane and in-phase superstrate, *Progress in Electromagnetics Research* **140** (2013) 147-167. 10.2528/PIER13040206.
19. Hakimi S., Rahim S. K. A., Abedian M., Noghabaei S., and Khalily M. - CPW-fed transparent antenna for extended ultrawideband applications, *IEEE Antennas and Wireless Propagation Letters* **13** (2014) 1251-1254. 10.1109/LAWP.2014.2333091.
20. Azini A. S., Kamarudin M. R., Rahman T. B. A., Iddi H. U., Abdulrahman A. Y., and Jamlos M. F. B. - Transparent antenna design for WiMAX application, *Progress In Electromagnetics Research* **138** (2013) 133-141. 10.2528/PIER13021809.